



# Optimizing Fast-Dissolving Tablets of Ketotifen. Impact of Sodium Bicarbonate and Citric Acid in Formulation and Evaluation

Rozhan Arif<sup>1</sup>, Sharad Visht<sup>1\*</sup>, Ali Omar Yassen<sup>1</sup>, Sana Sirwan Salih<sup>1</sup>

## Abstract

The research aimed to develop and assess fast-dissolving tablets (FDT) of ketotifen, a second-generation noncompetitive H<sub>1</sub>-receptor blocker, due to its poor oral bioavailability resulting from rapid first-pass effect (~50%) and poor solubility despite excellent permeability within the II-class of the biopharmaceutical classification system (BCS). The methodology involved formulating ketotifen with various excipients, including sodium bicarbonate, citric acid, menthol, polyvinyl pyrrolidone (PVP), aspartame, magnesium stearate, saccharin sodium, and dextrose. The combination of sodium bicarbonate and citric acid served as a fast-disintegrating agent by evolving carbon dioxide. Employing 23 factorial designs, the study assessed the impact of sodium bicarbonate (X1), citric acid (X2), and menthol (X3) on FDT performance. Batch A, exhibiting desirable characteristics, demonstrated weight variation (200±0.53), thickness (3.52±0.12 mm), hardness (2.87±0.23), friability (0.55±0.12), disintegration time (16±3 s), drug content uniformity (99.45±0.23), wetting time (3±1 s), and water absorption ratio (19.23±0.43). The

primary contributor to fast tablet disintegration was identified as the high concentration of sodium bicarbonate rather than citric acid. All batches adhered to the Peppas Korsmeyer model, signifying Fickian Diffusion (Higuchi Matrix) as the drug release mechanism. In conclusion, the study showed the pivotal role of sodium bicarbonate concentration in facilitating rapid tablet disintegration, emphasizing its significance over citric acid concentration.

**Keywords.** Fast-dissolving tablets (FDT), Ketotifen, Biopharmaceutical Classification System (BCS), Sodium Bicarbonate, Peppas Korsmeyer Model

## 1. Introduction

Ketotifen is a second generation noncompetitive H<sub>1</sub>-receptor blocker and stabilizes the mast cells (inverse agonist of H<sub>1</sub> receptor) on oral administration to avoid asthma attacks and other allergic reactions triggered by histamine release (Gandhi, 2022) (Bharkatiya et al., 2018) as showed in **Figure 1**. According to the biopharmaceutical classification system (BSC) It belongs to Class II (Truzzi et al., 2021), which means it has poor solubility and excellent permeability. It undergoes rapid first pass effect (~50%) results in the oral bioavailability that requires higher dose to meet the dosing requirements to patients to reach and maintain required therapeutic level (Aungst, 2017).

Several methods are available to improve drug dissolution to improve drug bioavailability, therapeutic effect, and fast disintegrating tablets (FDT) is one of the best approaches to improve efficiency, absorption, and bioavailability of drugs

**Significance** | The role of sodium bicarbonate concentration in facilitating rapid tablet disintegration, emphasizing its significance over citric acid concentration.

\*Correspondence. Dr. Sharad Visht, Assistant Professor, Department of Pharmaceutics, Faculty of Pharmacy, Tishk International University, Erbil, Kurdistan Region, Iraq. Mobile. +91-9719302784, E-mail. sharad.visht@tiu.edu.iq

Editor Md Shamsuddin Sultan Khan And accepted by the Editorial Board Jan 19, 2024 (received for review Nov 3, 2023)

## Author Affiliation.

<sup>1</sup> Department of Pharmaceutics, Faculty of Pharmacy, Tishk International University, Erbil, Kurdistan Region, Iraq.

## Please cite this article.

Rozhan Arif, Sharad Visht, Ali Omar et al., (2024). Optimizing Fast-Dissolving Tablets of Ketotifen. Impact of Sodium Bicarbonate and Citric Acid in Formulation and Evaluation, *Journal of Angiotherapy*, 8(1), 1-11, 9379

(Masih et al., 2017). The FDT provides rapid tablet disintegration/dissolution within a few seconds in a buccal cavity on hydration with saliva without need of water (Siddiqui et al., 2010). Also, oral administration is an easy and convenient route for drug administration (Alqahtani et al., 2021). FDT also sorts out the problem like dysphagia especially with pediatric and geriatric also some patients with disabilities (Gupta et al., 2010). Due to rapid disintegrate and drug release of FDT, the contents dissolve rapidly with in less than a min. and active ingredient exposed to pre-gastric absorption of drug also that facilitate the oral absorption of drug fraction from buccal cavity (Gupta et al., 2010), esophagus subsequently enhance bioavailability with the comparison to conventional tablets.

Orally fast dissolving tablets offer rapid absorption (Wolska et al., 2020), better bioavailability, and protection of active ingredients from first pass effect metabolism as medication passes through pre-gastric absorption and thus provide rapid drug action (Masih et al., 2017). In addition, FDT is convenient for patients (geriatric, pediatric, psychiatric, and bedridden) who have difficulty in swallowing caps/tablets, and at travelling or busy patients who can't avail water all the time for administration of conventional oral solid dosage forms (Muhammed R.A. et al., 2023) (Kashyap et al., 2011) (Masih et al., 2017). FDT also improves safety and eliminates the phobia of tablet swelling and vomit by decreasing the risk of choking or suffocation. It gives a good mouth feeling especially for bitter or unfavorable taste medications (Kashyap et al., 2011).

The excipients that found in formulation of mouth disintegrating tablets have great role in fast tablet disintegration, and mainly the required excipients are super-disintegrant like sodium starch glycolate (SSG), flavors like peppermint, anise oil, eucalyptus oil, thyme oil, sweeteners as fructose, lactitol, xylitol, sorbitol, binders like hydroxypropyl methylcellulose, polyvinyl alcohol, lubricants like stearic acid, zinc state, talc, polyethylene glycol, coloring agent like amaranth, Sunset yellow, and fillers like dextrose, sorbitol, mannitol. (Siraj et al., 2017) (Ayenew et al., 2009) (Sivapriya, 2018) There are conventional methods used to formulate orally fast dissolving/ disintegrating tablets such as freeze-drying method, phase transition, molding, spray drying, sublimation, melt granulation process, cotton candy process, mass extrusion, direct compression using super-disintegrant. Beside these methods some patented techniques like Zydis, Orosolv, Durasolv, Flashtab, wow tab, Flash dose also are available (Corveleyn & Remon, 1997) (Badgujar & Mundada, 2011).

As ketotifen bears low solubility and undergoes rapid first pass effect (~50%) on oral administration, the challenge was to improve the solubility of drug using hydrophilic excipient like dextrose as filler, sodium bicarbonate and citric acid combination as disintegrant, menthol as flavors, polyvinyl pyrrolidone (PVP) as

binder, aspartame as sweetener, magnesium stearate as lubricant, Sodium saccharin as sweetener in order to prepare the fast disintegrating tablet that may show improve solubility and bioavailability of drug (Ayenew et al., 2009) (Badgujar & Mundada, 2011).

### Materials And Methods

The ketotifen was the gifted sample form Awa medica, Erbil, Iraq. The sodium bicarbonate, citric acid, menthol, polyvinyl pyrrolidone (PVP), aspartame, magnesium stearate, saccharin sodium and dextrose procured from FINKEM. All chemicals were of analytical grades.

**Preformulation studies of ketotifen.** The melting point, UV and FTIR were performed to characterize and identify the drug ketotifen (Soltani et al., 2017).

**Melting point.** The capillary fusion method was used to measure the melting point of ketotifen using pre-calibrated (sodium bicarbonate AR and L-ascorbic acid AR) melting point apparatus. (Visht & Kulkarni, 2015) (Srivastava et al., 2010).

**Ultraviolet-visible spectrophotometer.** A double beam U. V. Spectrophotometer (Cintra 2020, GBC Scientific Equipment) used to determine the calibration data. The stock solution (1 mg/mL) was prepared by using buffer solution phosphate (pH 7.4) and further dilutions (10, 20, 30, 40, 50, 60, 70, 80, 90, 100 µg/mL) were prepared. The maximum absorbance ( $\lambda_{max}$ ) was determined, and absorbance of all prepared dilution was examined to prepare the calibration curve, absorbance vs concentrations (µg/mL) (Sharma et al., 2012).

**Fourier transform infrared spectroscopy.** The powdered moisture-free sample of ketotifen was scanned in range of 600 to 4000  $cm^{-1}$  to obtain Fourier transform infrared spectrum using IR spectrophotometer (FTIR 8400, Shimadzu, Kroyto, Japan) to determine the distinctive peaks of the several functional groups and bonds. (Sharma et al., 2012) (Visht & T Kulkarni, 2016).

**Drug excipient interaction.** The drug excipient compatibility confirmed by FTIR of drug excipients, their mixtures, and formulation.

**Composition of FDT of ketotifen.** The  $2^3$  factorial designs used to prepare the FDT of ketotifen to determine the influence of sodium bicarbonate and citric acid on performance of FDT. Three factors selected, named sodium bicarbonate as  $X_1$ , citric acid as  $X_2$  and menthol as  $X_3$ . The low and elevated levels were set as showed in Table 1.

**Pre-compression study of powder blend or micromeritics analysis.**

The bulk volume, true volume, bulk density, true density, void volume, porosity, angle of repose, Hausner's ratio and Carr's index were determined (Patel et al., 2020).

**Bulk density and tapped density.** The measuring cylinder filled with a precisely weighted amount of powder ( $W$ ), and the volume occupied by powder and measured as bulk volume ( $V_b$ ). The measuring cylinder filled with powder was manually tapped 100 times from a at 2 sec interval and height of 2.5 cm and the change in volume ( $V_F$ ) was noted to calculate bulk density ( $\rho_b$ ), true density ( $\rho_t$ ), void volume or pore volume and porosity respectively by following equation given below (Mehra et al., 2021) (Patel et al., 2020) (Mohan & Gundamaraju, 2015)

$$\rho_b = W / V_b$$

$$\rho_t = W / V_F$$

$$\text{Void volume (mL)} = (V_b - V_t)$$

Or

$$V_0 = (V_b - V_t)$$

$$\text{Porosity} = (V_0 / V_t)$$

**Flow properties by angle of repose ( $\theta$ ).** The funnel was filled with accurately weighed powder to make a heap to measure the height ( $h$ ) and radius ( $r$ ) to calculate the angle of repose as showed in Table2 using the following equation. (Gupta et al., 2013)

$$\tan \theta = h / r$$

$$\theta = \tan^{-1}(h/r)$$

**Carr's Compressibility index and Hausner's ratio.** The percentage of variance between the tapped and bulk density to tapped density is known as Carr's index while the ratio of tapped density to bulk density is Hausner's ratio as showed in Table3 (Shah et al., 2008).

$$\text{Carr's Index} = (\rho_t - \rho_b) * 100 / \rho_t$$

$$\text{Hausner's ratio} = \rho_t / \rho_b$$

**Preparation of FDT or formulation of fast dissolving tablets.** A Direct compression method utilized to formulate the FDTs of ketotifen. Accurately weighed quantities mixed in mortar pestle and mixed well to make a homogenous powder mass. The mass was compressed into tablets (Abd El Rasoul & Shazly, 2017).

**Evaluation of FDT or post-compression evaluation of fast dissolving tablet.** The drug content uniformity, hardness, thickness, wetting time, water absorption ratio, and drug release kinetics disintegration time drug release study were determined.

**Weight variation test.** Individual and average tablet weights calculated after randomly selecting twenty pills. The weight of each pill compared to the average weight of tablets. Tablets succeeded the weight variation test if the comparison of weight variation falls within the I.P limits (Sharma, 2013).

**Uniformity of thickness.** Thickness of 10 tablets were measured using Vernier caliper (Tukaram et al., 2010).

**Hardness test.** The YD-1 Tablet Hardness Tester (Made. Tian Jin Optical Instrumentation Factory) It was employed to evaluate the hardness of a tablet. in Newton (Patel et al., 2020).

**Friability test.** The CS-2 Friability Tester used to measure friability. A plastic chamber containing tablets placed in the friabilator that revolved for one hundred revolutions (4X25 rpm) and tablets dropped from six inches height on each revolution. The muslin cloth was used to de-dust the tablets, teeters were reweighed and friability ( $F\%$ ) was calculated by following formula. (Panigrahi et al., 2012).

$$F = (W_0 - W) * 100 / (W_0)$$

Where,

$W_0$  = Initial weight of the tablets (before the test)

$W$  = Weight of the tablets after the test

**Drug content uniformity.** The 5 tablets were ground into powder and weight equivalent to 5 mg of the drug was dissolved in ethanol and measured by double beam U. V. Spectrophotometer (Cintra 2020, GBC Scientific Equipment) at 210 nm (Karimi Afshar et al., 2022).

**Wetting time.** A petri plate containing a twice folded tissue paper soaked with 6 mL of water (37°C) and placed on Petri dish. The time was recorded for the complete wetting of the tablet. (Bharkatiya et al., 2018)

**Water absorption.** A twice folded tissue paper placed in a small 6 ml Petri dish containing of water, the tablet was set upon paper to examine the time required for complete wetting of the tablet. The weight of the wet tablet further measured. The following equation was used to calculate the water absorption ratio ( $R$ ). (Karimi Afshar et al., 2022)

$$R = 100 (W_a - W_b) / W_b$$

Where,

$R$  = Water absorption ratio

$W_a$  = Initial weight of dry tablet

$W_b$  = Weight of wet tablet

**In-vitro disintegration time.** The disintegration time was determined by placing a tablet in each tube (6 tubes) of the disintegration test apparatus and immersed in 0.1 N HCl (pH=1.2) maintained at 37±2°C. (Karimi Afshar et al., 2022)

**In-vitro dissolution studies.** The Type-II USP dissolution apparatus (Paddle type, Model. DIS8000) used to examine *in-vitro* dissolution. The 900 ml 0.1 N HCl (pH=1.2) set at 37±0.5 °C used as dissolution medium. Stirring speed was 100 rpm and sampling time were 1, 5, 10, 15, 30, 45, 60, 75, 90 min, the sample volume was 5 mL that replaced by addition of fresh buffer in dissolution media to maintain sink condition. The double beam UV Spectrophotometer used to measure the absorbance of samples to calculate % cumulative drug release vs time plot. The study was conducted in triplicate. (Bharkatiya et al., 2018)

**Drug release kinetics.** The kinetics drug release was determined for all batches to know the best fit model and mechanism of drug release.

**Stability study.** The optimized FDT formulation (Batch-A) analysed for drug content, wetting time, disintegration time to conduct stability study at  $25\pm 2^{\circ}\text{C}$ ,  $60\pm 5\% \text{RH}$ . Samples taken at 7, 14, 21 and 28 days.

## Results

### Preformulation studies of ketotifen

**Melting point.** The melting point (average) of ketotifen was  $191\pm 1.2^{\circ}\text{C}$ .

**UV-visible spectrophotometer.** The equation of line was  $Y=0.001X-0.000$  and  $r^2$  value 0.999 using the calibration data showed in Table 4 and calibration curve showed in Figure-2.

**Fourier Transform Infrared Spectroscopy.** The FTIR 8400 (Shimadzu, Kyoto, Japan) used to identify the functional groups and bonds present. The dried ketotifen powder loaded on FTIR window and scanned between range, and the range of spectra was determined to be 500 to  $4000\text{ cm}^{-1}$ , as showed in Figure-3. The distinctive values of the different functional groups have identified.

**Drug excipient interaction.** The FTIR of excipients and formulation was determined as showed in Figure-3.

**Ketotifen.** The FTIR of ketotifen showed the presence of C=C stretching at  $1678\text{ cm}^{-1}$ ,  $1665\text{ cm}^{-1}$ . Alkene aromatic C=C stretching vibration at  $1646\text{ cm}^{-1}$ ,  $1648\text{ cm}^{-1}$ . C=O at  $1388\text{ cm}^{-1}$ ,  $1651\text{ cm}^{-1}$ ,  $1717\text{ cm}^{-1}$ ,  $1722\text{ cm}^{-1}$ ,  $1725\text{ cm}^{-1}$ ,  $1732\text{ cm}^{-1}$ . C-C at  $1466\text{ cm}^{-1}$ ,  $1508\text{ cm}^{-1}$ ,  $1612\text{ cm}^{-1}$ . C-H  $\text{cm}^{-1}$  bending at  $2937\text{ cm}^{-1}$ . C-H rock at  $1379\text{ cm}^{-1}$ ,  $1385\text{ cm}^{-1}$ . C-H scissoring at  $1467\text{ cm}^{-1}$ ,  $1471\text{ cm}^{-1}$ . C-H stretching at  $736\text{ cm}^{-1}$ ,  $1057\text{ cm}^{-1}$ ,  $1088\text{ cm}^{-1}$ ,  $1385\text{ cm}^{-1}$ ,  $1451\text{ cm}^{-1}$ ,  $1469\text{ cm}^{-1}$ ,  $2724\text{ cm}^{-1}$ ,  $2829\text{ cm}^{-1}$ ,  $2862\text{ cm}^{-1}$ ,  $2875\text{ cm}^{-1}$ ,  $2876\text{ cm}^{-1}$ ,  $2927\text{ cm}^{-1}$ ,  $2963\text{ cm}^{-1}$ ,  $2972\text{ cm}^{-1}$ ,  $2975\text{ cm}^{-1}$ ,  $2984\text{ cm}^{-1}$ ,  $2994\text{ cm}^{-1}$ ,  $3031\text{ cm}^{-1}$ ,  $3066\text{ cm}^{-1}$ ,  $3075\text{ cm}^{-1}$ ,  $3098\text{ cm}^{-1}$ . C-H wagging at  $1273\text{ cm}^{-1}$ . C-N stretching at  $1235\text{ cm}^{-1}$ ,  $1337\text{ cm}^{-1}$ , N-H at  $1667\text{ cm}^{-1}$ ,  $3287\text{ cm}^{-1}$ ,  $3426\text{ cm}^{-1}$ ,  $3441\text{ cm}^{-1}$ ,  $3463\text{ cm}^{-1}$ , bending vibration  $\text{CH}_3$  at  $1475\text{ cm}^{-1}$ . OH at  $1395\text{ cm}^{-1}$  as showed in Figure-3.

**Sodium bicarbonate.** FTIR of sodium bicarbonate showed the presence of C-H at  $878\text{ cm}^{-1}$ ,  $904\text{ cm}^{-1}$ ,  $1426\text{ cm}^{-1}$ . O-H at  $1408\text{ cm}^{-1}$ ,  $3429\text{ cm}^{-1}$ ,  $3643\text{ cm}^{-1}$ . C=O at  $1674\text{ cm}^{-1}$ ,  $1774\text{ cm}^{-1}$ . C-O at  $1065\text{ cm}^{-1}$  as showed in Figure-3.

**Citric acid.** The FTIR of citric acid showed the presence of C=O at  $1715\text{ cm}^{-1}$ ,  $1724\text{ cm}^{-1}$ ,  $1729\text{ cm}^{-1}$ ,  $1731\text{ cm}^{-1}$ . COOH group at  $3000\text{ cm}^{-1}$ – $3100\text{ cm}^{-1}$ . C-O at  $1167\text{ cm}^{-1}$ ,  $1205\text{ cm}^{-1}$ . O-H at  $1651\text{ cm}^{-1}$ . C-C at  $1467\text{ cm}^{-1}$ ,  $1505\text{ cm}^{-1}$ ,  $1617\text{ cm}^{-1}$ . C-H scissoring at  $1466\text{ cm}^{-1}$ ,  $1473\text{ cm}^{-1}$ . C-H rock at  $1378\text{ cm}^{-1}$ ,  $1387\text{ cm}^{-1}$ . C-H stretching at  $1389\text{ cm}^{-1}$ ,  $2973\text{ cm}^{-1}$ ,  $1472\text{ cm}^{-1}$ ,  $1054\text{ cm}^{-1}$ ,  $734\text{ cm}^{-1}$ ,  $1087\text{ cm}^{-1}$ ,  $1452\text{ cm}^{-1}$ ,  $2989\text{ cm}^{-1}$ ,  $2973\text{ cm}^{-1}$ ,  $2992\text{ cm}^{-1}$ ,  $2975\text{ cm}^{-1}$ ,  $2963\text{ cm}^{-1}$ ,  $2924\text{ cm}^{-1}$ ,  $3098\text{ cm}^{-1}$ ,  $3066\text{ cm}^{-1}$ ,  $3031\text{ cm}^{-1}$ ,  $2875\text{ cm}^{-1}$ ,  $2829\text{ cm}^{-1}$ ,  $2724\text{ cm}^{-1}$ . C-H wagging at  $1275\text{ cm}^{-1}$  as showed in Figure-3.

**Menthol.** The FTIR of menthol showed the presence of OH at  $3395\text{ cm}^{-1}$ ,  $2888\text{ cm}^{-1}$ . C-H at  $1163\text{ cm}^{-1}$ , C-O group at  $3714\text{ cm}^{-1}$ ,

O-H at  $3263\text{ cm}^{-1}$ ,  $\text{CH}_2$  *asy* stretch at  $2954\text{ cm}^{-1}$ ,  $\text{CH}_2$  *sy-str.* at  $2926\text{ cm}^{-1}$ . C-C at  $1466\text{ cm}^{-1}$ ,  $1508\text{ cm}^{-1}$ ,  $1612\text{ cm}^{-1}$ . C-H at  $2882\text{ cm}^{-1}$ ,  $1472\text{ cm}^{-1}$ ,  $1385\text{ cm}^{-1}$ ,  $2974\text{ cm}^{-1}$ ,  $1472\text{ cm}^{-1}$ ,  $1058\text{ cm}^{-1}$ ,  $737\text{ cm}^{-1}$ ,  $3075\text{ cm}^{-1}$ ,  $2927\text{ cm}^{-1}$ ,  $3064\text{ cm}^{-1}$ ,  $3039\text{ cm}^{-1}$ ,  $2872\text{ cm}^{-1}$  as showed in Figure-3.

**Polyvinylpyrrolidone.** The FTIR of polyvinylpyrrolidone showed the presence of C=O at  $1353\text{ cm}^{-1}$ ,  $1268\text{ cm}^{-1}$ ,  $1725\text{ cm}^{-1}$  strong,  $1719\text{ cm}^{-1}$  strong,  $1733\text{ cm}^{-1}$  strong,  $1728\text{ cm}^{-1}$ ,  $1652\text{ cm}^{-1}$ ,  $1643\text{ cm}^{-1}$ ,  $1427\text{ cm}^{-1}$ . C-C at  $1467\text{ cm}^{-1}$ ,  $1504\text{ cm}^{-1}$ ,  $1617\text{ cm}^{-1}$ . C-H bending at  $2965\text{ cm}^{-1}$ . C-H scissoring at  $1473\text{ cm}^{-1}$ . C-H rock at  $1377\text{ cm}^{-1}$ ,  $1381\text{ cm}^{-1}$ . C-H stretching at  $1385\text{ cm}^{-1}$ ,  $2875\text{ cm}^{-1}$ ,  $2953\text{ cm}^{-1}$ ,  $2974\text{ cm}^{-1}$ ,  $1472\text{ cm}^{-1}$ ,  $1058\text{ cm}^{-1}$ ,  $737\text{ cm}^{-1}$ ,  $3076\text{ cm}^{-1}$ ,  $2923\text{ cm}^{-1}$ ,  $3096\text{ cm}^{-1}$ ,  $2876\text{ cm}^{-1}$ ,  $2722\text{ cm}^{-1}$ ,  $1275\text{ cm}^{-1}$ . C-N  $1323\text{ cm}^{-1}$ ,  $2984\text{ cm}^{-1}$ ,  $1238\text{ cm}^{-1}$ ,  $1656\text{ cm}^{-1}$ ,  $1284\text{ cm}^{-1}$ . OH at  $3391\text{ cm}^{-1}$ , at  $1376\text{ cm}^{-1}$ . C-N, at  $1012\text{ cm}^{-1}$ . N-H stretching  $1647$ ,  $1587\text{ cm}^{-1}$  as showed in Figure-3.

**Aspartame.** The FTIR of aspartame showed the presence of C=C at  $1655\text{ cm}^{-1}$ ,  $1645\text{ cm}^{-1}$ . O-H at  $3077\text{ cm}^{-1}$ , C=O at  $1298\text{ cm}^{-1}$ ,  $1727\text{ cm}^{-1}$ . Carbonyl group at  $1655\text{ cm}^{-1}$ . C-C at  $1506\text{ cm}^{-1}$ ,  $1615\text{ cm}^{-1}$ ,  $1465\text{ cm}^{-1}$ . C-H bending at  $2893\text{ cm}^{-1}$ . C-H scissoring at  $1462\text{ cm}^{-1}$ ,  $1472\text{ cm}^{-1}$ . C-H rock at  $1377\text{ cm}^{-1}$ ,  $1385\text{ cm}^{-1}$ . C-H stretching at  $1382\text{ cm}^{-1}$ ,  $2876\text{ cm}^{-1}$ ,  $2973\text{ cm}^{-1}$ ,  $1472\text{ cm}^{-1}$ ,  $1057\text{ cm}^{-1}$ ,  $736\text{ cm}^{-1}$ ,  $3077\text{ cm}^{-1}$ ,  $3035\text{ cm}^{-1}$ ,  $2726\text{ cm}^{-1}$ ,  $1275\text{ cm}^{-1}$ . C-N at  $2984\text{ cm}^{-1}$ ,  $1247\text{ cm}^{-1}$ . N-H at  $1314\text{ cm}^{-1}$ . O-H at  $3545\text{ cm}^{-1}$ . N-H stretching (primary amine) at  $3514\text{ cm}^{-1}$ ,  $3358\text{ cm}^{-1}$ . COOH carboxylic acid at  $3200\text{ cm}^{-1}$ – $2700\text{ cm}^{-1}$ . N-H stretching of amine salt at  $2973\text{ cm}^{-1}$ . O=C=O stretching at  $2349\text{ cm}^{-1}$ . C=O stretching aldehyde at  $1735\text{ cm}^{-1}$ ,  $1727\text{ cm}^{-1}$  as showed in Figure-3.

**Mg-stearate.** The FTIR of magnesium stearate showed the presence of C=O at  $1269\text{ cm}^{-1}$ ,  $1721\text{ cm}^{-1}$ ,  $1715\text{ cm}^{-1}$ ,  $1731\text{ cm}^{-1}$ ,  $1726\text{ cm}^{-1}$ . C-C at  $1506\text{ cm}^{-1}$ ,  $1465\text{ cm}^{-1}$ . C-H bending, at  $2937\text{ cm}^{-1}$ . C-H scissoring at  $1465\text{ cm}^{-1}$ ,  $1470\text{ cm}^{-1}$ . C-H rock at  $1378\text{ cm}^{-1}$ ,  $1383\text{ cm}^{-1}$ . C-H stretching at  $1383\text{ cm}^{-1}$ ,  $2879\text{ cm}^{-1}$ ,  $1470\text{ cm}^{-1}$ ,  $1055\text{ cm}^{-1}$ ,  $735\text{ cm}^{-1}$ ,  $1086\text{ cm}^{-1}$ ,  $2725\text{ cm}^{-1}$ ,  $1271\text{ cm}^{-1}$ . Carboxylic acid, metal-carboxylate at  $1699\text{ cm}^{-1}$  as showed in Figure-3.

**Saccharin sodium.** The FTIR of Saccharin sodium showed the presence of C=C stretching  $1652\text{ cm}^{-1}$ ,  $1659\text{ cm}^{-1}$ ,  $1656\text{ cm}^{-1}$ . O-H at  $3132\text{ cm}^{-1}$ . C=O at  $1278\text{ cm}^{-1}$ ,  $1723\text{ cm}^{-1}$ ,  $1715\text{ cm}^{-1}$ ,  $1731\text{ cm}^{-1}$ ,  $1650\text{ cm}^{-1}$ . C-C at  $1506\text{ cm}^{-1}$ ,  $1465\text{ cm}^{-1}$ ,  $1614\text{ cm}^{-1}$ . C-H bend at  $2987\text{ cm}^{-1}$ , C-H scissoring at  $1465\text{ cm}^{-1}$ ,  $1470\text{ cm}^{-1}$ . C-H rock at  $1378\text{ cm}^{-1}$ ,  $1383\text{ cm}^{-1}$ . C-H stretching at  $1383\text{ cm}^{-1}$ ,  $2879\text{ cm}^{-1}$ ,  $2863\text{ cm}^{-1}$ ,  $2971\text{ cm}^{-1}$ ,  $1470\text{ cm}^{-1}$ ,  $1055\text{ cm}^{-1}$ ,  $735\text{ cm}^{-1}$ ,  $1450\text{ cm}^{-1}$ ,  $2986\text{ cm}^{-1}$ ,  $2991\text{ cm}^{-1}$ ,  $2976\text{ cm}^{-1}$ ,  $2961\text{ cm}^{-1}$ . C-N  $1277\text{ cm}^{-1}$ ,  $3923\text{ cm}^{-1}$ . C=O at  $1643\text{ cm}^{-1}$ . Benzene ring stretching of C-C group at  $1585\text{ cm}^{-1}$ ,  $1458\text{ cm}^{-1}$ ,  $1336\text{ cm}^{-1}$ ,  $1257\text{ cm}^{-1}$ ,  $1149\text{ cm}^{-1}$ . The  $-\text{SO}_2$  stretching vibrations  $968\text{ cm}^{-1}$ ,  $748\text{ cm}^{-1}$ . S=O stretching at  $1397\text{ cm}^{-1}$ ,  $1385\text{ cm}^{-1}$ . C=O stretching at  $1673\text{ cm}^{-1}$ . C=C bending at  $1000\text{ cm}^{-1}$ – $650\text{ cm}^{-1}$ . C-N stretching at  $1342\text{ cm}^{-1}$ – $1266\text{ cm}^{-1}$  as showed in Figure-3.

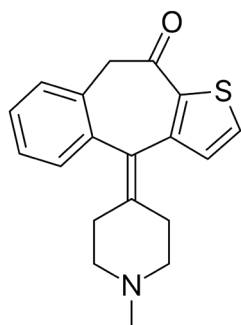


Figure 1. Structure of ketotifen

Table 1. Composition of FDT (2<sup>3</sup> Experimental design) of Ketotifen tablets

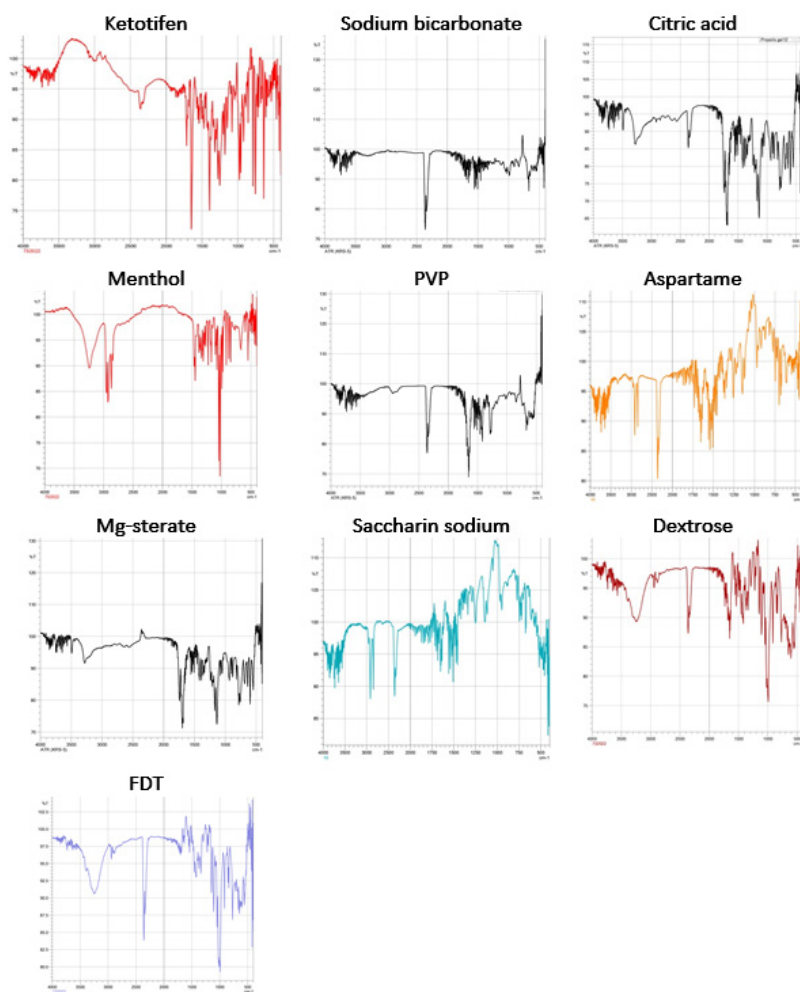
Ingredients		Ingredients						
Ketotifen (mg)		1						
Sodium bicarbonate (mg)		X <sub>1</sub>						
Citric acid (mg)		X <sub>2</sub>						
Menthol (mg)		X <sub>3</sub>						
PVP (mg)		50						
Aspartam (mg)		1						
Mg-sterate		10						
Saccharin sodium (mg)		1						
Dextrose (mg) q.s.		200						
<b>Levels</b>								
	<b>Low (-)</b>	<b>Mid</b>		<b>High (+)</b>				
X <sub>1</sub>	50	55		84				
X <sub>2</sub>	15	20		25				
X <sub>3</sub>	5	10		15				
<b>Batches</b>								
	X <sub>1</sub>	X <sub>2</sub>		X <sub>3</sub>				
A	+	+		+				
B	+	-		+				
C	-	+		+				
D	+	+		-				
E	+	-		-				
F	-	+		-				
G	-	-		+				
H	-	-		-				
<b>Ingredients</b>								
	A	B	C	D	E	F	G	H
Ketotifen (mg)	1	1	1	1	1	1	1	1
Sodium bicarbonate (mg)	84	84	50	84	84	50	50	50
Citric acid (mg)	25	15	25	25	15	25	15	15
Menthol (mg)	15	15	15	5	5	5	15	5
PVP (mg)	50	50	50	50	50	50	50	50
Aspartam (mg)	5	5	5	5	5	5	5	5
Mg-sterate	10	10	10	10	10	10	10	10
Saccharin sodium (mg)	10	10	10	10	10	10	10	10
Dextrose (mg) q.s. 200	0	10	34	10	20	44	44	54
<b>Total</b>	200	200	200	200	200	200	200	200

Table 2. Angle of Repose and flow properties of Ketotifen tablets

Angle of Repose (°)	Type of Flow
Less than 20	Excellent
Between 20 – 30	Good
Between 30 – 34	Passable
More than 34	Very Poor

**Table 3.** Hausner’s Ratio and Carr’s Index of Ketotifen tablets

Flow properties	Hausner's Ratio	Carr's Index
Excellent/ Very Free Flow	1-11.1	<10
Good/ Free Flow	11.2-11.8	1 - 15.0
Fair	11.9-12.5	16-20
Passable	12.6-13.4	24-25
Poor Flow/ Cohesive	13.5-14.5	26-31
Very Poor Flow/ Very Cohesive	14.6-15.9	32-37
Approximate no Flow	>16	>38



**Figure 3.** FTIR of excipients and formulation of Ketotifen tablets

**Dextrose.** The FTIR of dextrose showed the presence of OH Stretch at 3277 cm<sup>-1</sup>, 3682 cm<sup>-1</sup>, 1116 cm<sup>-1</sup>. Esters group at 1177 cm<sup>-1</sup>. C-O stretching at 1293 cm<sup>-1</sup>, 1267 cm<sup>-1</sup>. C-C at 1504 cm<sup>-1</sup>, 1465 cm<sup>-1</sup>, 1612 cm<sup>-1</sup>. C-H bending at 2976 cm<sup>-1</sup>. C-H scissoring at 1462 cm<sup>-1</sup>, 1473 cm<sup>-1</sup>. C-H rock at 1375 cm<sup>-1</sup>, 1382 cm<sup>-1</sup>, 2876 cm<sup>-1</sup>, 2865 cm<sup>-1</sup>, 2973 cm<sup>-1</sup>, 1472 cm<sup>-1</sup>, 1053 cm<sup>-1</sup>, 739 cm<sup>-1</sup>, 1083 cm<sup>-1</sup>, 3076 cm<sup>-1</sup>, 1451 cm<sup>-1</sup>, 2983 cm<sup>-1</sup>, 2973 cm<sup>-1</sup>, 2995 cm<sup>-1</sup>, 2973 cm<sup>-1</sup>, 2964 cm<sup>-1</sup>, 2922 cm<sup>-1</sup>, 3097 cm<sup>-1</sup>, 3067 cm<sup>-1</sup>, 3036 cm<sup>-1</sup>, 2875 cm<sup>-1</sup>, 2824 cm<sup>-1</sup>, 2726 cm<sup>-1</sup>, 1273 cm<sup>-1</sup> as showed in Figure-3.

**FTIR of FDT.** The FTIR of FDT showed the presence of C-C at 1150 cm<sup>-1</sup>, 1258 cm<sup>-1</sup>, 1339 cm<sup>-1</sup>, 1456 cm<sup>-1</sup>, 1467 cm<sup>-1</sup>, 1507 cm<sup>-1</sup>, 1586 cm<sup>-1</sup>, 1619 cm<sup>-1</sup>. C=C at 1576 cm<sup>-1</sup>, 1654 cm<sup>-1</sup>, 1675 cm<sup>-1</sup>. C=O at 1266 cm<sup>-1</sup>, 1355 cm<sup>-1</sup>, 1425 cm<sup>-1</sup>, 1645 cm<sup>-1</sup>, 1656 cm<sup>-1</sup>, 1729 cm<sup>-1</sup>, 1735 cm<sup>-1</sup>. C-O at 1165 cm<sup>-1</sup>, 1206 cm<sup>-1</sup>, 1296 cm<sup>-1</sup>, 3717 cm<sup>-1</sup>. C-H at 738 cm<sup>-1</sup>, 876 cm<sup>-1</sup>, 905 cm<sup>-1</sup>, 1055 cm<sup>-1</sup>, 1166 cm<sup>-1</sup>, 1277 cm<sup>-1</sup>, 1383 cm<sup>-1</sup>, 1424 cm<sup>-1</sup>, 1468 cm<sup>-1</sup>, 2827 cm<sup>-1</sup>, 2873 cm<sup>-1</sup>, 2966 cm<sup>-1</sup>, 2997 cm<sup>-1</sup>, 3033 cm<sup>-1</sup>, 3037 cm<sup>-1</sup>, 3065 cm<sup>-1</sup>, 3078 cm<sup>-1</sup>, 3094 cm<sup>-1</sup>. Esters group at 1177 cm<sup>-1</sup>. COOH at 3494 cm<sup>-1</sup>. O=C=O stretching at 2346 cm<sup>-1</sup>. Carboxylic acid, metal-carboxylate at 1699 cm<sup>-1</sup>. CH at 2952 cm<sup>-1</sup>, CH<sub>2</sub> at 2923 cm<sup>-1</sup>. CH<sub>2</sub> *asy* stretch at 2952 cm<sup>-1</sup>. CH<sub>2</sub> *sy-str.* at 2928 cm<sup>-1</sup>. CH<sub>3</sub> at 1477 cm<sup>-1</sup>. C-N at 1014 cm<sup>-1</sup>, 1232 cm<sup>-1</sup>, 1236 cm<sup>-1</sup>, 1244 cm<sup>-1</sup>, 1276 cm<sup>-1</sup>, 1287 cm<sup>-1</sup>, 1325 cm<sup>-1</sup>, 1334 cm<sup>-1</sup>, 1652 cm<sup>-1</sup>, 2985 cm<sup>-1</sup>, 2987 cm<sup>-1</sup>, 3925 cm<sup>-1</sup>. N-H at 1317 cm<sup>-1</sup>, 1589 cm<sup>-1</sup>, 1644 cm<sup>-1</sup>, 1668 cm<sup>-1</sup>, 2976 cm<sup>-1</sup>, 3289 cm<sup>-1</sup>, 3355 cm<sup>-1</sup>, 3428 cm<sup>-1</sup>, 3445 cm<sup>-1</sup>, 3467 cm<sup>-1</sup>, 3514 cm<sup>-1</sup>. O-H at 1118 cm<sup>-1</sup>, 1377 cm<sup>-1</sup>, 1393 cm<sup>-1</sup>, 1407 cm<sup>-1</sup>, 1655 cm<sup>-1</sup>, 2882 cm<sup>-1</sup>, 3075 cm<sup>-1</sup>, 3135 cm<sup>-1</sup>, 3268 cm<sup>-1</sup>, 3273 cm<sup>-1</sup>, 3396 cm<sup>-1</sup>, 3398 cm<sup>-1</sup>, 3424 cm<sup>-1</sup>, 3546 cm<sup>-1</sup>, 3647 cm<sup>-1</sup>, 3686 cm<sup>-1</sup>. S=O stretching at 1395 cm<sup>-1</sup>, 1388 cm<sup>-1</sup>. -SO<sub>2</sub> stretching vibrations at 967 cm<sup>-1</sup>, 745 cm<sup>-1</sup> as showed in Figure-3.

### Pre-compression study of powder blend

Total eight batches of powder blends were prepared and evaluated for bulk and true density, void volume, porosity, angle of repose, Hausner's ratio, compressibility index (CI) / Carr's index and were determined as tabulated in Table 5.

### Evaluation of FDT or Post-compression Evaluation of Fast Dissolving Tablet

Total eight batches of tablets were prepared and evaluated. The weight variation varied between 200±0.35 to 200±0.76, thickness varied between 3.51±0.12 to 3.54±0.13 mm, hardness varied between 2.81±0.14 to 2.89±0.21, friability varied between 0.34±0.24 to 0.64±0.2, disintegration Time varied between 16±2 to 23±4, drug content uniformity varied between 99.34±0.34 to 99.98±0.12, wetting time (s`ec) varied between 3±1 to 15±2 and water absorption ratio varied between 19.23±0.43 to 27.34±0.24 as showed in Table 5, Figure 4A, 4B, 4C. Batch A showed the disintegration time 99.45±0.23 s, wetting time 3±1 s and water absorption ratio 19.23±0.43 s.

### In-vitro Dissolution Studies

The drug release studies indicated that the Batch A showed the maximum drug release 94.23% at 75 min. The high amount of sodium bicarbonate and citric acid was the basic reason behind high drug release as showed in Table 6 and Figure 7. Amount of sodium bicarbonate matters for high disintegration due to formation of carbon dioxide in acidic medium in stomach and citric acid. The concentration of sodium bicarbonate plays more key role as compared to citric acid in dissolution of tablets found in a study by Mohamed A.O. and Ali A. S., 2018. The P-value was 0.93293 using ANOVA test as showed in Table 8. The F-score is <1, the variance between the samples is no greater than the variance within the samples and the samples probably come from populations with the same mean.

### Drug release kinetics

All FDT batches prepared by direct compression method showed the Peppas Korsmeyer model as the best fit model. One study by Mushtaq et al, 2021 also found the best fit model for drug release from FDT was Korsmeyer-Peppas model. The result of drug release kinetics was similar. The mechanism of drug release was Fickian Diffusion (Higuchi Matrix) as showed in Table 8.

### Stability Studies

The optimized FDT formulation (Batch A) showed no significance change in drug content, wetting time, disintegration time. The drug content was 99.56±0.23, wetting time was 3±2.2 and disintegration time was 17±1.7 at 28 weeks at 25±2°C, 60±5%RH as showed in Table 9.

### Discussion

Ketotifen, a second-generation noncompetitive H<sub>1</sub>-receptor blocker, is utilized to stabilize mast cells, acting as an inverse agonist of H<sub>1</sub> receptors. This is particularly relevant in preventing asthma attacks and allergic reactions triggered by histamine release. However, ketotifen belongs to Class II of the biopharmaceutical classification system (BCS), characterized by poor solubility and excellent permeability. Additionally, it undergoes a rapid first-pass effect, resulting in poor oral bioavailability. The primary objective of the research was to formulate fast-dissolving tablets (FDT) of ketotifen to address these challenges and improve its therapeutic effectiveness.

### Significance of Fast-Dissolving Tablets

Fast-dissolving tablets (FDT) present a promising solution for improving drug dissolution, bioavailability, and therapeutic effects. These tablets disintegrate rapidly in the buccal cavity upon hydration with saliva, eliminating the need for water during administration. FDTs offer several advantages, including rapid

**Table 5.** Evaluation of FDT of Ketotifen tablets

Parameters	A	B	C	D	E	F	G	H
Weight Variation	200±0.53	200±0.76	200±0.47	200±0.35	200±0.64	200±0.56	200±0.47	200±0.75
Thickness	3.52±0.12	3.54±0.13	3.51±0.12	3.54±0.11	3.53±0.1	3.52±0.11	3.51±0.13	3.54±0.12
Hardness	2.87±0.23	2.87±0.13	2.81±0.14	2.89±0.16	2.89±0.21	2.83±0.23	2.81±0.14	2.83±0.12
Friability	0.55±0.12	0.34±0.24	0.63±0.2	0.52±0.1	0.46±0.14	0.47±0.23	0.56±0.12	0.64±0.2
Disintegration Time (s)	16±3	17±4	21±3	16±2	18±3	22±3	23±4	23±2
Drug content uniformity	99.45±0.23	99.34±0.34	99.97±0.11	99.43±0.32	99.75±0.21	99.85±0.22	99.68±0.43	99.98±0.12
Wetting time (s)	3±1	6±2	9±1	5±1	8±1	11±2	13±1	15±2
Water absorption ratio	19.23±0.43	22.45±0.13	24.23±0.27	20.22±0.34	23.12±0.23	25.34±0.12	26.21±0.43	27.34±0.24
Average Bulk volume	5.3	5.33	5.3	5.5	5.46	5.17	5.27	5.17
Average True volume	4.73	4.67	4.43	4.8	4.7	4.6	4.37	4.43
Bulk density	7.55	7.5	7.55	7.27	7.32	7.74	7.59	7.74
True density	8.45	8.57	9.02	8.33	8.51	8.7	9.16	9.02
Void volume	0.57	0.67	0.87	0.7	0.77	0.57	0.9	0.73
Porosity (%)	0.07	0.08	0.1	0.08	0.09	0.07	0.1	0.08
Angle of repose (θ)	18.3	18.3	17.7	17.2	17.2	17.2	17.7	17.2
Carr's index	7.56	7.7	8.19	7.46	7.65	7.81	8.33	8.16
Hausner's index	1.12	1.14	1.2	1.15	1.16	1.12	1.21	1.17

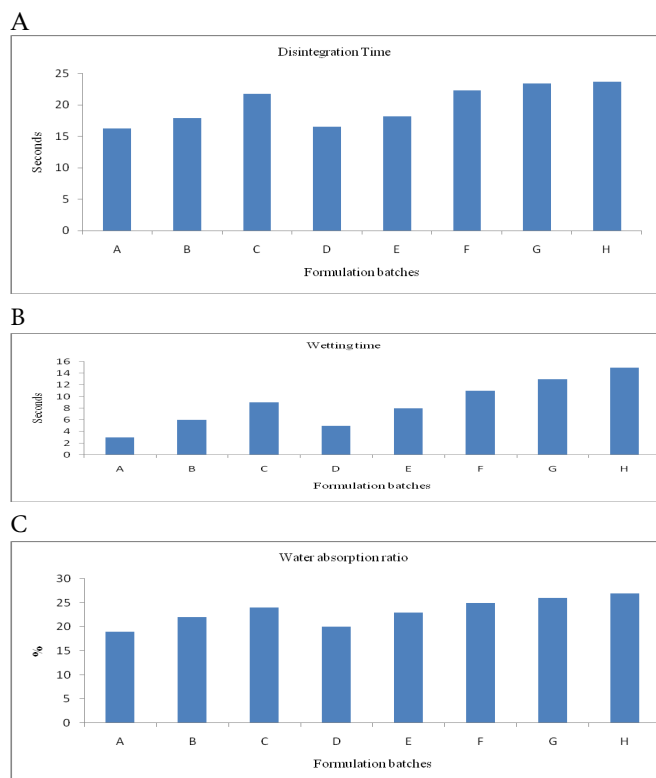


**Figure 4.** A) Disintegration Time (Sec) of FDT, B) Wetting time (Sec) of FDT, C) Water absorption ratio of FDT of Ketotifen tablets.



**Table 6.** Drug dissolution study of Ketotifen tablets

Time (Min)	A	B	C	D	E	F	G	H
0	0	0	0	0	0	0	0	0
1	38.05±1.23	34.75±0.97	24.82±1.34	33.09±1.32	29.78±0.97	26.47±1.45	26.47±1.17	23.16±1.26
10	64.56±1.13	62.91±0.76	54.64±0.58	62.91±0.67	57.95±1.13	51.33±1.12	49.67±1.25	46.36±0.75
30	92.18±0.75	90.53±1.42	82.25±1.23	90.53±0.86	85.56±1.35	78.95±0.45	77.29±1.32	73.98±1.32
60	94.26±1.56	92.61±0.87	84.34±1.11	92.61±1.34	87.65±0.76	81.03±1.34	79.37±0.76	76.06±0.56
75	94.23±0.87	92.59±1.25	84.3±0.76	92.61±0.79	87.63±1.22	81.01±0.63	79.34±1.23	76.06±0.67

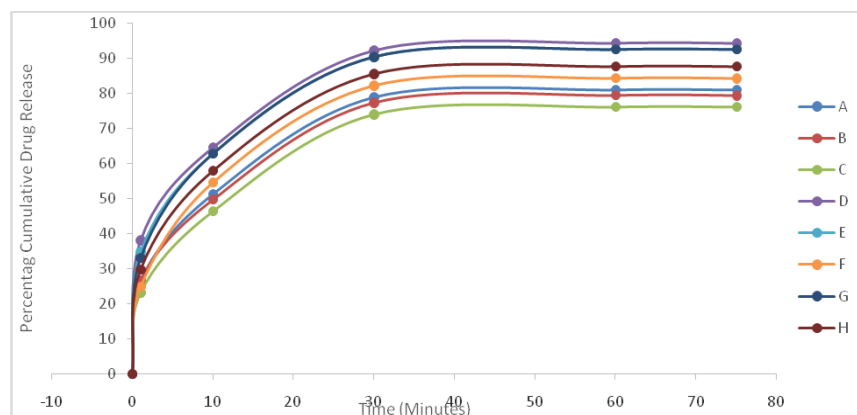


**Figure 7.** Drug release data of FDTs of Ketotifen tablets

**Table 7.** ANOVA Summary of statistical analysis of Ketotifen tablets

Source	DF	SS	MS	F-Stat	P-Value
Between Groups	7	1466.84	209.55	0.33	0.93293
Within Groups	32	20143.8	629.49		
Total	39	21610.6			

**Table 8.** Drug release kinetics of different formulatiomn of Ketotifen tablets

	A		B		C		D		E		F		G		H	
	R <sup>2</sup>	K	R <sup>2</sup>	K	R <sup>2</sup>	K	R <sup>2</sup>	K	R <sup>2</sup>	K	R <sup>2</sup>	K	R <sup>2</sup>	K	R <sup>2</sup>	K
<b>Zero order</b>	0.649 0	0.973 5	0.659 3	0.973 2	0.691 0	0.934 4	0.663 6	0.982 7	0.676 6	0.944 6	0.692 8	0.887 7	0.695 0	0.8687	0.708 1	0.849 8
<b>1st order</b>	0.835 2	- 0.036 7	0.826 1	- 0.033 4	0.802 4	- 0.023 5	0.827 0	- 0.033 6	0.808 7	- 0.026 5	0.797 2	- 0.020 8	0.795 1	-0.0196	0.794 7	- 0.017 9
<b>Higuchi Matrix</b>	0.940 8	9.832 5	0.939 4	9.802 4	0.937 4	9.515 7	0.939 1	9.838 9	0.937 6	9.607 9	0.935 7	9.269 0	0.935 1	9.1628	0.934 4	9.029 4
<b>Peppas</b>	0.971 1	4.903 0	0.970 1	4.731 9	0.965 7	4.130 0	0.968 5	4.647 9	0.969 2	4.438 6	0.970 6	4.203 5	0.970 9	4.1904	0.970 8	3.964 3
<b>Hix.Crow.</b>	0.784 4	0.007 4	0.780 2	0.007 0	0.770 6	0.005 6	0.781 6	0.007 0	0.771 7	0.006 0	0.767 5	0.005 1	0.766 7	0.0049	0.769 8	0.004 6
<b>Best fit model=</b>	Peppas Korsmeyer		Peppas Korsmeyer		Peppas Korsmeyer		Peppas Korsmeyer		Peppas Korsmeyer		Peppas Korsmeyer		Peppas Korsmeyer		Peppas Korsmeyer	
<b>n =</b>	0.2209		0.2378		0.2949		0.2490		0.2615		0.2721		0.2679		0.2896	
<b>k =</b>	4.9030		4.7319		4.1300		4.6479		4.4386		4.2035		4.1904		3.9643	
<b>Mechanism of release</b>	Fickian Diffusion (Higuchi Matrix)															

**Table 9.** Drug content of FDT (Batch A) in stability studies of Ketotifen tablets

Time (Weeks)	Drug content	Wetting time (sec)	Disintegration time (sec)
0	99.99±0.61	3±1	16±1.2
7	99.98±0.31	3±1	16±1.3
14	99.98±0.22	3±1.5	16±1.5
21	99.97±0.33	3±2.1	17±1.5
28	99.56±0.23	3±2.2	17±1.7

absorption, enhanced bioavailability, and convenience of administration. They are particularly beneficial for patients with difficulties in swallowing conventional tablets, including pediatric, geriatric, psychiatric, and bedridden individuals. Additionally, the rapid disintegration of FDTs facilitates pre-gastric absorption, leading to improved drug bioavailability.

#### Excipients and Formulation Methods

The formulation of FDTs involves the use of various excipients, each contributing to specific properties of the tablet. In this study, sodium bicarbonate, in combination with citric acid, menthol, polyvinyl pyrrolidone (PVP), aspartame, magnesium stearate, saccharin sodium, and dextrose, played a crucial role. Sodium bicarbonate and citric acid acted as a fast-disintegrating agent by evolving carbon dioxide, promoting rapid tablet dissolution. The research utilized a 23 factorial design to explore the influence of sodium bicarbonate, citric acid, and menthol on FDT performance.

#### Preformulation Studies

Preformulation studies, including the determination of the melting point, UV-visible spectrophotometry, and Fourier Transform Infrared Spectroscopy (FTIR), were conducted to understand the physical and chemical properties of ketotifen. These studies provided essential information on the drug's characteristics, aiding in the selection of suitable excipients for the formulation.

#### Evaluation of FDTs

Post-compression evaluations of the formulated tablets involved a comprehensive analysis of various parameters, including weight variation, thickness, hardness, friability, disintegration time, drug content uniformity, wetting time, water absorption ratio, and in-vitro drug release kinetics. Among the eight batches, Batch A exhibited optimal characteristics, with a weight variation of  $200 \pm 0.53$ , disintegration time of  $16 \pm 3$  seconds, and a maximum in-vitro drug release of 94.23% at 75 minutes.

#### Influence of Sodium Bicarbonate and Citric Acid

The results indicated that the concentration of sodium bicarbonate played a pivotal role in the fast disintegration of the tablet, overshadowing the influence of citric acid concentration. This observation underscores the significance of excipient selection, particularly in achieving rapid drug release.

#### Drug Release Kinetics

All FDT batches followed the Peppas Korsmeyer model as the best fit model for drug release kinetics, indicating a consistent and predictable release pattern. The mechanism of drug release was identified as Fickian Diffusion (Higuchi Matrix), reinforcing the reliability of the formulations.

#### Stability Studies

Stability studies conducted over 28 weeks on the optimized FDT formulation (Batch A) demonstrated no significant changes in

drug content, wetting time, or disintegration time. This highlights the robustness of the formulation under specified storage conditions, reinforcing its potential for long-term use.

#### Conclusion

In conclusion, among the eight batches of fast-dissolving tablets formulated in this study, Batch A emerged as the most promising due to its rapid disintegration and maximum drug release. The high concentration of sodium bicarbonate was identified as the major factor influencing fast tablet disintegration, with citric acid playing a lesser role. The Peppas Korsmeyer model consistently described the drug release kinetics, and the mechanism of drug release was identified as Fickian Diffusion. This research emphasizes the critical role of excipients, especially sodium bicarbonate, in formulating FDTs with enhanced therapeutic potential. The developed FDTs, particularly Batch A, hold promise as a viable alternative for the treatment and prevention of asthmatic attacks. The study contributes valuable insights into the formulation of FDTs, providing a foundation for further advancements in drug delivery technologies.

#### Author contribution

S.V. prepared study design, A.O., R.A. conceptualized, S.S.S. performed experimental and data analysis

#### Acknowledgment

The authors thank the management of TIU to provide every facility for the conduct of this research.

#### Competing financial interests

The authors have no conflict of interest.

#### Symbols and Abbreviations

**BCS.** Biopharmaceutical classification system; **PVP.** polyvinyl pyrrolidone; **FDT.** Fast-dissolving tablets; **sec.** Second; **L.** Litre; **mL.** Milliliter; **Min.** Minutes; **AR.** Analytical Reagent; **U.V..** Ultraviolet; **μ.** Micro; **g.** Gram; **FTIR.** Fourier transform infrared; **ρ.** Density; **θ.** Theta; **I.P.** Indian Pharmacopoeia; **%.** Percentage; **N.** Normal; **°.** Degree; **C.** Centigrade; **RH.** Relative humidity; **CI.** Carr's index or compressibility index; **ANOVA.** Analysis of variance.

#### References

- Abd El Rasoul, S., & Shazly, G. A. (2017). Propafenone HCl fast dissolving tablets containing subliming agent prepared by direct compression method. *Saudi Pharmaceutical Journal*, 25(7), 1086-1092.
- Alqahtani, M. S., Kazi, M., Alsenaidy, M. A., & Ahmad, M. Z. (2021). Advances in oral drug delivery. *Frontiers in Pharmacology*, 12, 618411.

- Aungst, B. J. (2017). Optimizing oral bioavailability in drug discovery. an overview of design and testing strategies and formulation options. *Journal of pharmaceutical sciences*, 106(4), 921-929.
- Aynew, Z., Puri, V., Kumar, L., & Bansal, A. K. (2009). Trends in pharmaceutical taste masking technologies. a patent review. *Recent patents on drug delivery & formulation*, 3(1), 26-39.
- Badgular, B., & Mundada, A. (2011). The technologies used for developing orally disintegrating tablets. A review. *Acta pharmaceutica*, 61(2), 117-139.
- Bharkatiya et al., 2018 technology. *International Journal of Pharmaceutical & Biological Archives*, 1(1), 1-10.
- Bharkatiya, M., Kitawat, S., & Gaur, K. (2018). Formulation and characterization of fast dissolving tablet of salbutamol sulphate. *American Journal of Pharmacological Sciences*, 6(1), 1-6.
- Corveleyn, S., & Remon, J. P. (1997). Formulation and production of rapidly disintegrating tablets by lyophilisation using hydrochlorothiazide as a model drug. *International journal of pharmaceutics*, 152(2), 215-225.
- Gandhi, I. T. (2022). The effect of treatment with the mast cell stabilizer ketotifen fumarate on chronic widespread pain in teenagers. McGill University (Canada).
- Gupta, A., Mishra, A., Gupta, V., Bansal, P., Singh, R., & Singh, A. (2010). Recent trends of fast dissolving tablet-an overview of formulation
- Gupta, R., Sharma, P., Garg, A., Soni, A., Sahu, A., Rai, S., Rai, S., & Shukla, A. (2013). Formulation and evaluation of herbal effervescent granules incorporated with *Calliandra haematocephala* leaves extract. *Indo American Journal of Pharmaceutical Research*, 3(6), 4366-4371.
- Karimi Afshar, S., Abdorashidi, M., Dorkoosh, F. A., & Akbari Javar, H. (2022). Electrospun fibers. Versatile approaches for controlled release applications. *International Journal of Polymer Science*, 2022.
- Kashyap, S., Sharma, V., & Singh, L. (2011). Fast disintegrating tablet. A boon to pediatric and geriatric. *International Journal of Pharma Professional's Research (IJPPR)*, 2(2), 266-274.
- Masih, A., Kumar, A., Singh, S., & Tiwari, A. K. (2017). Fast dissolving tablets. A review. *Int J Curr Pharm Res*, 9(2), 8-18.
- Mehra, P., Kapoor, V., Gupta, N., Rajpoot, D. S., & Sharma, N. (2021). Formulation evaluation and characterization of fast dissolving tablets of Rofecoxib. *Research Journal of Topical and Cosmetic Sciences*, 12(1), 60-64.
- Mohamed, A.O., & Ali A. S. (2018). Preparation and Evaluation of Rapidly Dissolving Tablet of Telmisartan. *Journal of advanced pharmacy research*, 2 (3), 191-200
- Mohan, A., & Gundamaraju, R. (2015). In vitro and in vivo evaluation of fast-dissolving tablets containing solid dispersion of lamotrigine. *International journal of pharmaceutical investigation*, 5(1), 57.
- Muhammed, R.A., Yalman Othman, Z., Rashid Noaman, B., Visht, S., Jabbar, S., & Sirwan Salih, S. (2023). Innovations In Formulation And Evaluation Of Oral Fast Dissolving Film. *Eurasian Journal of Science and Engineering*, 9(2).
- Mushtaq, M., Fazal, N., & Niaz, A. (2021). Correction to. Formulation and Evaluation of Fast-Disintegrating Tablets of Flurbiprofen and Metoclopramide. *J Pharm Innov* 16, 439-440. <https://doi.org/10.1007/s12247-020-09461-1>
- Panigrahi, R., Chowdary, K., Mishra, G., Bhowmik, M., & Behera, S. (2012). Formulation of fast dissolving tablets of Lisinopril using combination of synthetic superdisintegrants. *Asian Journal of Pharmacy and Technology*, 2(3), 94-98.
- Patel, Z., Bhura, R., & Shah, S. (2020). Formulation optimization and evaluation of mouth dissolving film of ramosetron hydrochloride. *Int J Curr Pharm Sci*, 12, 99-105.
- Shah, R. B., Tawakkul, M. A., & Khan, M. A. (2008). Comparative evaluation of flow for pharmaceutical powders and granules. *AAPS PharmSciTech*, 9, 250-258.
- Sharma, D. (2013). Formulation development and evaluation of fast disintegrating tablets of salbutamol sulphate for respiratory disorders. *International Scholarly Research Notices*, 2013.
- Sharma, K., Agrawal, S., & Gupta, M. (2012). Development and validation of UV spectrophotometric method for the estimation of curcumin in bulk drug and pharmaceutical dosage forms. *Int. J. Drug Dev. Res*, 4(2), 375-380.
- Siddiqui, M. N., Garg, G., & Sharma, P. K. (2010). Fast dissolving tablets. preparation, characterization and evaluation. an overview. *International Journal of Pharmaceutical Sciences Review and Research*, 4(2), 87-96.
- Siraj, S. N., Kausar, S. H., Khan, G., & Khan, T. (2017). Formulation and evaluation of oral fast dissolving tablet of ondansetron hydrochloride by coprocess excipients. *Journal of Drug Delivery and Therapeutics*, 7(5), 102-108.
- Sivapriya, S. (2018). Formulations and Evaluation of Oral Dispersible Tablets of Lafutidine by Direct Compression Method College of Pharmacy, Madurai Medical College, Madurai.
- Soltani, S., Zakeri-Milani, P., Barzegar-Jalali, M., & Jelvehgari, M. (2017). Fabrication and in-vitro evaluation of ketotifen fumarate-loaded PLGA nanoparticles as a sustained delivery system. *Iranian journal of pharmaceutical research. IJPR*, 16(1), 22.
- Srivastava, P., Malviya, R., & Visht, S. (2010). Formulation development and evaluation of atenolol fast disintegrating tablets for treatment of hypertension. *JChrDD*, 1(1), 36-42.
- Truzzi, F., Tibaldi, C., Zhang, Y., Dinelli, G., & D' Amen, E. (2021). An overview on dietary polyphenols and their biopharmaceutical classification system (BCS). *International journal of molecular sciences*, 22(11), 5514.
- Tukaram, B. N., Rajagopalan, I. V., & Shartchandra, P. S. I. (2010). The effects of lactose, microcrystalline cellulose and dicalcium phosphate on swelling and erosion of compressed HPMC matrix tablets. texture analyzer. *Iranian journal of pharmaceutical research. IJPR*, 9(4), 349.
- Visht, S., & Kulkarni, G. (2015). Studies on the Preparation and in vitro-in vivo Evaluation of Mucoadhesive Microspheres of Glycyrrhetic Acid Isolated from Liquorice. *Bangladesh Pharmaceutical Journal*, 18(1), 30-37.
- Visht, S., & T Kulkarni, G. (2016). Glycyrrhetic Acid Ammonium Loaded Microspheres Using *Colocasia esculenta* and *Bombax ceiba* mucilages. *In Vitro and In Vivo Characterization. Current Drug Therapy*, 11(2), 101-114.
- Wolska, E., Sznitowska, M., Krzemirska, K., & Ferreira Monteiro, M. (2020). Analytical techniques for the assessment of drug-lipid interactions and the active substance distribution in liquid dispersions of solid lipid microparticles (SLM) produced de novo and reconstituted from spray-dried powders. *Pharmaceutics*, 12(7), 664.